NEOPLASIA
www.neoplasia.com

Volume 11 Number 8 August 2009 pp. 780–792 780

Development, Characterization, and Immunotherapeutic Use of Peptide Mimics of the Thomsen-Friedenreich Carbohydrate Antigen[1]

Jamie Heimburg-Molinaro[*,2], Adel Almogren[†], Susan Morey[‡], Olga V. Glinskii[§], Rene Roy[¶], Gregory E. Wilding[#], Richard P. Cheng[**], Vladislav V. Glinsky[††,‡‡] and Kate Rittenhouse-Olson[*,‡]

*Department of Microbiology and Immunology, University at Buffalo, The State University of New York, Buffalo, NY 14214, USA; [†]Immunopathology & Allergy Research, College of Medicine, King Saud University, Riyadh, Saudi Arabia; [‡]Department of Biotechnical and Clinical Laboratory Sciences, University at Buffalo, The State University of New York, Buffalo, NY 14214, USA; [§]Department of Medical Pharmacology and Physiology, University of Missouri, Columbia, MO 65211, USA; [¶]Department of Chemistry, University of Quebec at Montreal, Montreal, Quebec, Canada H3C 3P8; [#]Department of Biostatistics, University at Buffalo, The State University of New York, Buffalo, NY 14214, USA; **Department of Chemistry, National Taiwan University, Taipei 10617, Taiwan; [††]Department of Pathology and Anatomical Sciences, University of Missouri, Columbia, MO 65211, USA; [‡‡]Harry S. Truman Memorial Veterans Hospital, Columbia, MO 65201, USA

Abstract

The tumor-associated carbohydrate Thomsen-Friedenreich antigen (TF-Ag; Galβ1-3GalNAcα-*O*-Ser/Thr) is overexpressed on the cell surface of several types of tumor cells, contributing to cancer cell adhesion and metastasis to sites containing TF-Ag–binding lectins. A highly specific immunoglobulin G_3 monoclonal antibody (Ab) developed to TF-Ag (JAA-F11) impedes TF-Ag binding to vascular endothelium, blocking a primary metastatic step and providing a survival advantage. In addition, in patients, even low levels of antibodies to TF-Ag seem to improve prognosis; thus, it is expected that vaccines generating antibodies toward TF-Ag would be clinically valuable. Unfortunately, vaccinations with protein conjugates of carbohydrate tumor-associated Ags have induced clinically inadequate immune responses. However, immunization using peptides that mimic carbohydrate Ags such as Lewis has resulted in both Ab and T-cell responses. Here, we tested the hypothesis that vaccinations with unique TF-Ag peptide mimics may generate immune responses to TF-Ag epitopes on tumor cells, useful for active immunotherapy against relevant cancers. Peptide mimics of TF-Ag were selected by phage display biopanning using JAA-F11 and rabbit anti–TF-Ag Ab and were analyzed *in vitro* to confirm TF-Ag peptide mimicry. *In vitro*, TF-Ag peptide mimics bound to TF-Ag–specific peanut agglutinin and blocked TF-Ag–mediated rolling and stable adhesion of cancer cells to vascular endothelium. *In vivo*, the immunization with TF-Ag–mimicking multiple antigenic peptides induced TF-Ag–reactive Ab production. We propose that this novel active immunotherapy approach could decrease tumor burden in cancer patients by specifically targeting TF-Ag–positive cancer cells and blocking metastasis.

Neoplasia (2009) 11, 780–792

Abbreviations: Ab, antibody; Ag, antigen; MAP, multiple antigenic peptide; Ova, ovalbumin; PNA, peanut agglutinin; SPR, surface plasmon resonance; TF-Ag, Thomsen-Friedenreich antigen

Address all correspondence to: Dr. Kate Rittenhouse-Olson, Department of Biotechnical and Clinical Laboratory Sciences, 44 Cary Hall, 3635 Main St, Buffalo, NY 14214.
E-mail: krolson@buffalo.edu

[1]The authors thank the Department of Defense Breast Cancer Research Program Predoctoral Fellowship (J.H.-M.) and the National Institute of Allergy and Infectious Disease grant R15 AI 49210-01 for financial support (K.R.-O.). V.V.G. was supported by the funds from the VA BLR&D Service. O.V.G. was supported by the American Heart Association grant 0830287N. R.R. is also thankful to the Natural Sciences and Engineering Research Council of Canada for a Canada Research Chair in therapeutic chemistry.

[2]Current address: Department of Biochemistry, Emory University, Atlanta, GA.

Received 19 March 2009; Revised 22 April 2009; Accepted 24 April 2009

DOI 10.1593/neo.09504

Introduction

The tumor-associated carbohydrate antigen (Ag) Thomsen-Friedenreich (TF-Ag) is present on tumor cells including those of breast, lung, colon, bladder, and prostate [1–5]. TF-Ag, the core 1 disaccharide Galβ1-3GalNAcα-*O*-Ser/Thr [1–3], remains cryptic on normal cell membranes, covered by extended carbohydrate residues preventing exposure of the epitope to the immune system [1–3], but becomes exposed on cancer cell surfaces. An important role for TF-Ag has been recognized in the process of cell adhesion and metastasis [1–7]. TF-Ag binding moieties were found in sites of metastasis, offering an explanation for the correlation between TF-Ag surface expression on cancer cells and tumor aggressiveness and metastasis [4,6,7].

The human antibody (Ab) repertoire is known to contain low levels of anti–TF-Ag antibodies, mainly of the immunoglobulin (Ig) M isotype [1,2,8–12]. Patients with higher levels of anti–TF-Ag Ab have a better prognosis than patients with lower levels [1,2,8–13]. Thus, it seems that naturally formed antibodies to TF-Ag may have a beneficial effect even at relatively low levels. Additional indications that anti–TF-Ag could be clinically important come from animal experiments on spontaneous breast cancer metastasis, in which Ab to TF-Ag blocked metastasis and improved survival [6]. Thus, the fact that some patients generate Ab responses to TF-Ag that could be associated with better prognosis inspires research into active immunization approaches to supply anti–TF-Ag Ab to the patient.

Attempts to make Ab to TF-Ag in cancer patients began with a TF-Ag vaccine composed of blood group type O-MN red blood cell–derived glycoproteins, which resulted in improved breast cancer patient survival, although only small amounts of IgM Ab were produced [14]. Studies with protein conjugates of Ags related to TF-Ag, Tn, and sialyl Tn in colon cancer and sialyl Tn in breast cancer patients [15–18] induced low level Ab responses, which were still IgM-dominant, and some clinical responses were observed in these patients. These results, although promising, indicated no memory development, whereas one of the main reasons to use active immunization rather than passive transfer is the anticipation of long-term memory induction for protection from recurrences.

Peptide mimicry offers an alternative method for increasing carbohydrate Ag immunogenicity [19–21]. In cellular immunologic responses to peptide mimics and subsequent cytotoxic responses, recent results show that T cells primed by peptide mimics can subsequently react with carbohydrate moieties, potentially inducing cellular responses against carbohydrate epitope-bearing tumor cells [22–27], indicating that vaccinations with peptide mimics may be able to generate improved responses to carbohydrate epitopes on tumor cells. Kieber-Emmons et al. [22] and Luo et al. [23] used mimicry of Lewis Ags by peptides to induce enhanced immune responses and elicited T-cell–dependent *versus* T-cell–independent responses to the Ag [22,23]. In addition, studies with peptide mimics of bacterial carbohydrate Ags showed structural data supporting the ability of peptides to mimic carbohydrate Ags, and these mimics were prepared as conjugates for vaccine studies against the bacteria [28–30].

It seems that generation of an active immune response to TF-Ag using peptide mimics holds the potential to be clinically useful in conjunction with current therapies and, unlike passive transfer of Ab, to prevent long-term recurrence by generating an effective immune memory in the patient. For these reasons, the focus of our study was on developing and characterizing peptides that function as mimics of the TF-Ag structure *in vitro* with the ultimate goal of using these peptide mimics in vaccines for stimulating responses to TF-Ag.

Materials and Methods

Mimotope Selection, Phage Amplification, and Titering

Biopanning of phage expressing 12-mer peptides (New England Biolabs, Ipswitch, MA) [31,32] was performed on 96-well plates (Immulon; Dynatech Laboratories, Chantilly, VA) coated with partially purified JAA-F11 monoclonal Ab to Galβ1-3GalNAcα [3], for rounds 1 and 2. Round 3 of biopanning was performed on plates coated with partially purified rabbit polyclonal Ab to Galβ1-3GalNAc-α, which was created through immunization with a Galβ1-3GalNAcα-*O*-diazophenyl–BSA conjugate, with the specificity described by Diakun et al. [33]. The specificity of the JAA-F11 has been described in detail by Chaturvedi et al. [34], and its production was described in Rittenhouse-Diakun et al. [3]. Both antibodies require both the Gal and the GalNAc for binding, a free 3-hydroxyl on the galactose was required by both for binding, but neither Ab required a free 6-hydroxyl on the galactose nor on the *N*-acetyl-galactosamine, and lastly, both Ab preparations preferred the Galβ1-3GalNAc-α linked to the Galβ1-3GalNAc-β–linked structures. Nonspecific binding was blocked with 5 mg/ml BSA. Initially, 2×10^{12} phage per milliliter were added to the wells and incubated for 45 minutes. Unbound phages were removed with 10 washes of TBST (50 mM pH 7.5, Tris with Tween 20). Bound phages were eluted with 10 mM TF-Ag disaccharide for 10 minutes with rocking at room temperature (RT). Pooled selected phages were amplified and titered according to the manufacturer's protocols [31]. Final selection of positive mimicking clones was performed using JAA-F11 Ab on transfer immunoblots from titer plates.

In Vitro *Testing of Phage Mimicry*

Immunoblot analysis. Ten microliters of phage dilutions was applied to a TBS-wetted nitrocellulose membrane using a slot blot apparatus (BioRad, Hercules, CA) and blocked with 1% BSA-TBS. Primary Ab or lectin (JAA-F11, mouse IgG_3 isotype control, rabbit anti–TF-Ag, or peanut agglutinin [PNA]; Vector Laboratories, Burlingame, CA) was added and incubated for 1 to 2 hours. Immunoblot analysis proceeded according to the manufacturer's (Promega, Madison, WI) protocol using an alkaline phosphatase secondary Ab followed by the 5-bromo-4-chloro-3-indolyl phosphate/nitro blue tetrazolium substrate in the case of the antibodies and, in the case of PNA, by using an Ab to PNA followed by an alkaline phosphatase–conjugated secondary Ab and substrate [35]. Analysis was performed using densitometry (GS-700 Imaging Densitometer; Biorad).

Inhibition ELISA. ELISA microtiter plates (Immulon) were coated with 5 μg/ml TF-Ag–BSA conjugate in sodium bicarbonate buffer for 3 hours at 37°C. Plates were washed three times, and an inhibiting agent (selected phage) was mixed with equal volumes of primary Ab and incubated for 1 to 2 hours at 37°C. The mixture was added to the plate and incubated at 37°C for 1 to 2 hours. After washing, anti-mouse IgG alkaline phosphatase conjugate (Sigma, St. Louis, MO) was added and incubated at RT. After washing, *para*-nitrophenyl phosphate substrate (Sigma) was added. After incubation, the plate was read at 405 nm. Inhibition ELISAs were performed with JAA-F11, rabbit Ab to TF-Ag, and PNA mixed with phage.

Phage DNA Purification and Sequencing

DNA was purified from individual phage clones by an adaptation of standard protocol for DNA purification from M13 phage [31,36].

The 36-bp insert of interest was identified and translated to determine the unique 12–amino acid sequence of the selected phage. Peptides were produced containing the 12 amino acids plus the next three residues at the C-terminus in the phage sequence (GGG), and a cysteine or serine residue was added for conjugation purposes.

Solid-Phase Peptide Synthesis and Analysis

Solid-phase peptide synthesis (SPPS) was used to produce 16–amino acid peptides with Fmoc-based chemistry using standard protocols [37,38]. The peptides were purified using reverse-phase high-performance liquid chromatography (HPLC) on a Vydac C18 column (Grace Davison, Deerfield, IL). The purity of the peptides was confirmed by analytical HPLC, and the identity was confirmed by matrix-assisted laser desorption/ionization–time of flight. Additional peptides were purchased from Sigma-Genosys (The Woodlands, TX) and Bio-Synthesis, Inc (Lewisville, TX). Multiple antigenic peptides (MAPs) were produced by SPPS using Fmoc chemistry onto a branched lysine core resulting in eight 15-mer peptides presented on one structure (Figure 1; Bio-Synthesis, Inc). Previous studies have successfully produced TF-Ag conjugated to the MAP core [39,40]. Inhibition ELISAs was used to test ability of single peptide mimics to inhibit binding of Ab to TF-Ag as previously mentioned. Six different MAPs were produced as described, five containing selected TF-Ag mimicking sequences and one containing a negative control, using an ovalbumin (Ova) sequence (Table 1). Peptides were stored at −20°C under nitrogen in lyophilized form. Corresponding linear peptides were used in ELISAs.

Surface Plasmon Resonance Using Biacore

Binding kinetics were determined by surface plasmon resonance (SPR) using a BIACORE X biosensor system (Biacore, Piscataway, NJ) and defined experimental design [41,42]. JAA-F11 Ab to TF-Ag was immobilized on CM5 dextran sensor chips using amine-coupling chemistry reagents (Biacore). Approximately 10,000 resonance units (RUs) of JAA-F11 was immobilized, providing an active surface of 3000 to 4000 RU corresponding to 3000 to 4000 pg/mm^2. All measurements were carried out in HBS-EP buffer (0.01 M HEPES pH 7.4, 0.15 M NaCl, 3 mM EDTA, 0.005% surfactant P20; Biacore). Surface interactions were performed at 25°C at flow rates of 5 or 10 μl/min using a reference cell *versus* an experimental cell. RU values for Ag binding ranged from 5 to 250. Surface regeneration was performed using 10 mM HCl or 10 mM glycine pH 2.0 at 50 μl/min. Kinetic parameters for the binding of JAA-F11 to peptide D2 were determined using the BIAevaluation programs.

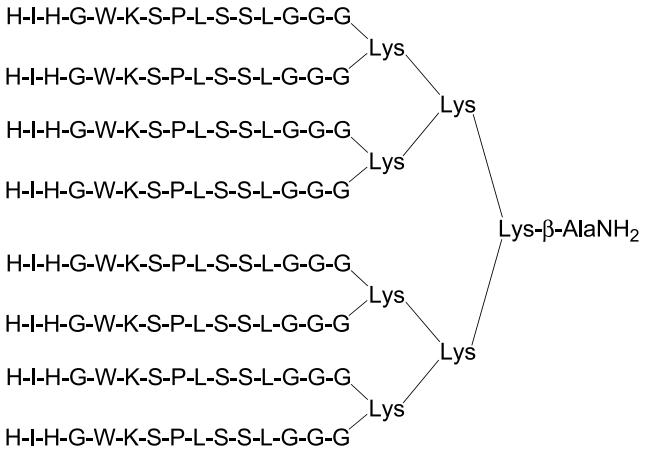

Figure 1. The structure of the D2 MAPs that were produced by SPPS using Fmoc chemistry onto a branched lysine core resulting in eight 15-mer peptides presented on one structure. Other peptide MAPs were prepared similarly.

Table 1. Sequence of MAP Peptides and Immunization Groups.

Group	MAPs (Eight 15–Amino Acid Peptides Linked to Lys Core)
1	D2 (HIHGWKSPLSSLGGG)
2	B3 (GHPHYITHKPNRGGG)
3	C1 (YPSLPVYHSLRSGGG)
4	*B1 (HHSHKTNLATTPGGG)
5	D1 (MHKPWSGHMQVPGGG)
6	Ova (SIINFEKLGAGAGGG)
7	Mixed MAP
8	PBS control

*Sequence B1 was obtained three times; clones C2 and D3 also contained this sequence (not listed).

In Vitro *Adhesion Assays*

Cell lines and cultures. The MDA-MB-435 human metastatic cancer cell line was kindly provided by Dr. J.E. Price (MD Anderson Cancer Center). MDA-MB-435 cells were maintained on plastic in 5% CO_2/95% air using the RPMI-1640 medium supplemented with L-glutamine, 10% fetal bovine serum, sodium pyruvate, and nonessential amino acids. The HBME-1 human bone marrow endothelial cell line was kindly provided by Dr. K.J. Pienta (University of Michigan) and grown as previously described [43].

In vitro *parallel flow chamber assay.* The adhesion of MDA-MB-435 cells to HBME-1 monolayers was studied *in vitro* with and without inhibitory molecules in a parallel plate laminar flow chamber as described previously [44]. Data are presented as the means ± SD of two independent experiments.

Prediction of Major Histocompatibility Complex Binding

SYFPEITHI [45], BIMAS [46], and RANKPEP [47] databases were used for major histocompatibility complex (MHC) binding algorithms.

Sequence Homology

The Basic Local Alignment Search Tool (BLAST) database was used [48] for sequence comparison to known proteins. The amino acid sequences were entered into the protein short, nearly exact sequence comparison database using limitation to *Homo sapiens* and *Mus muscularus* organism sequences.

Immunization Protocols

A vaccination protocol involving 200 Balb/c mice divided evenly into eight groups was used (Table 1). All blood draws were obtained by retro-orbital bleed, under 3% isoflurane anesthesia. To prepare each vaccination mixture, 3 mg of MAP was dissolved in 1.5 ml of sterile-filtered PBS (2 mg/ml) and, 1.2 ml of Alum adjuvant (aluminum hydroxide at 40 mg/ml; Pierce) was added dropwise. After mixing for 30 minutes, 0.3 ml of inactivated *Bordetella pertussis* suspension at 200 × 10^9 organisms per milliliter (Wako Chemicals, Richmond, VA) was added to the tube and mixed to homogeneity. One hundred microliters was injected into each mouse, divided into four sites at the back. Thus, each mouse received 100 μg of MAP plus 1.6 mg of Alum and 2 × 10^9 *B. pertussis* organisms as adjuvant per

immunization [49,50]. A primary vaccination and three booster immunizations at 2-week intervals were given to each mouse. After the prebleed, four additional blood draws were obtained, 2 weeks after each immunization (Table 1). All animal experimentation was done using approved institutional protocols, in a facility approved by the Association for Assessment and Accreditation of Laboratory Animal Care.

Serum Analysis

Indirect ELISAs were performed on Immulon microtiter plates: for the first group of mice, sera from all five blood draws from each of the 200 mice were tested for IgG and IgM Abs in triplicate on both TF-Ag–BSA–coated plates (1:50), on linear peptide–coated plates (1:200, 1:400, and 1:800) corresponding to the MAP used for immunization and on Ova linear peptide–coated plates for IgG and IgM Abs (1:200, 1:400, and 1:800). Sera dilutions were incubated for 2 hours at 37°C; the plates were washed three times with 1× TBS-Brij, and anti–mouse IgG alkaline phosphatase conjugate (1:1000; Sigma) was added and incubated at RT for 1 hour. The plates were washed three times as previously, and *p*-nitrophenyl phosphate substrate (Sigma) was added for 1 hour, after which the plates were read at 405 nm on a spectrophotometer. The plates were washed three times as previously mentioned, and anti–mouse IgM–horseradish peroxidase conjugate (1:4000; Sigma) was added to each plate and incubated for 1 hour at RT. The plates were washed three times and *O*-phenylenediamine substrate (Sigma) was added for 1 hour and read at 450 nm.

Statistical Analyses

The averages of the triplicates were determined for each mouse in each group and used as the unit of analysis. Groups were then compared by Student's *t* tests. This allowed for comparison of the Ab levels from preimmunization to weeks 6 and 8 within each group, as well as the levels between groups. To simplify the analysis, the higher value of week 6 or week 8 was used as the postimmunization level comparisons. In the analysis of the serum Ab response by enzyme immunoassays, to describe the observed variability in the data and test for difference between groups, a mixed linear model was fit to each end point, optical density (OD) IgG, and OD IgM. Once the model was fit, specific linear contrasts based on the model parameters were constructed and used to test for mean differences between the two control groups (Ova and PBS) and each of the six experimental groups (B1, B3, C1, D1, D2, and Mix) at both 6 and 8 weeks. To control for multiple testing, Bonferroni-adjusted *P* values were computed for all 24 hypothesis tests, thereby bounding the experiment-wise error rate at 0.05 per end point. Standard diagnostic tools were used to assess model fit. Also computed for each end point was the response rate by group based on the absolute change for a variety of cut points. Microsoft Excel (Microsoft, Redmond, WA), Minitab Release 14 (Minitab, Inc., State College, PA), and SAS version 9.0 statistical software (SAS, Cary, NC) were used for all analyses. Standard diagnostic plots for normal-based models were used in all analyses, and model fit was deemed adequate.

Results

Biopanning, Mimic Isolation, and Selection

Biopanning with mouse monoclonal Ab and rabbit Ab eluted with TF-Ag decreased the likelihood of nonspecific binding to Ab. To carry out successful biopanning, a titer of 1 to 2×10^9 plaque-forming units (PFUs)/100 μl or greater was required with high stringency conditions. The percent recovery of binding phage increased with each round of biopanning. Final phage amplification and selection were performed with immunoprobing of titered phage followed by positive phage amplifications.

Amplification of isolated phage was needed to obtain a sufficient amount of phage for subsequent experiments. The phage pellet was titered to determine the number of PFUs. Successful phage titers, appearing as plates with well-separated colonies, were obtained using dilutions from 1×10^5 to 1×10^{11}. Typical titers were in the range of 3 to 5×10^9 PFU/ml.

To isolate phage containing TF-Ag mimics, a transfer of phage to nitrocellulose from Luria Bertani plates with well-separated colonies was performed, and the membrane was incubated with JAA-F11 Ab to TF-Ag, followed by anti–mouse enzyme-conjugated Ab and corresponding substrate for color development. Specific colonies corresponding to phage mimics appeared purple, whereas phage that did not mimic, as well as wild-type phage, appeared white. Positive colonies were plucked from the titer plates and amplified again to generate distinct positive phage clones that mimic TF-Ag.

Immunoblot analysis. To analyze phage pools selected by biopanning, four immunoblots were performed. The pooled phage mixture blotted at different concentrations on nitrocellulose was probed with JAA-F11 Ab (Figure 2*A*), rabbit polyclonal anti–TF-Ab (Figure 2*B*), or PNA, a TF-Ag–binding lectin (Figure 2*C*). In each case, the immunoblot demonstrated specific binding to the positive phage pool and not to the negative phage pool. Next, the phage pool was probed with an isotype control IgG_3 Ab, 4A11, specific for pneumococcal saccharide, compared with JAA-F11 binding (Figure 2*D*). These experiments demonstrated that pooled phage contained specific phage isolates able to mimic TF-Ag and bind mouse monoclonal anti–TF-Ag JAA-F11 Ab, rabbit polyclonal anti–TF-Ag Ab, and TF-Ag–specific PNA but not a control Ab.

Individual phage clones were selected using transfer immunoblots, in which positively reacting phage were plucked and amplified to produce individual positive phage clones. Figure 2 shows the blot quantitation of five individual phage clones and their reactivity with JAA-F11 Ab (Figure 2*E*), rabbit Ab to TF-Ag (Figure 2*F*), and PNA lectin (Figure 2*G*). Phage clones were tested at the following: B1 and B3—5×10^9 PFU/ml, C1 and D2—4×10^9 PFU/ml, D1—3×10^9 PFU/ml, E—6×10^{13} PFU/ml. A representative of multiple experiments is shown. These experiments show that selected individual phage clones are creating a peptide conformation similar enough to TF-Ag to bind TF-Ag–specific Abs and lectin, supporting the theory that they mimic TF-Ag.

Inhibition ELISA. To further show that selected phage clones do mimic TF-Ag, inhibition ELISA was performed using JAA-F11 Ab. Phage inhibited JAA-F11 binding to TF-Ag–coated plates by varying amounts (Table 2). D2 phage showed the highest amount of inhibition (49%). These experiments indicated that three of the five phage clones at 5 μg/ml in solution bound JAA-F11 well enough to prevent binding of JAA-F11 to TF-Ag, the original target carbohydrate Ag. A representative of three experiments is shown.

Phage Sequencing

To identify the peptides that were able to mimic TF-Ag in immunoblot analysis and inhibition ELISA experiments, the selected phage

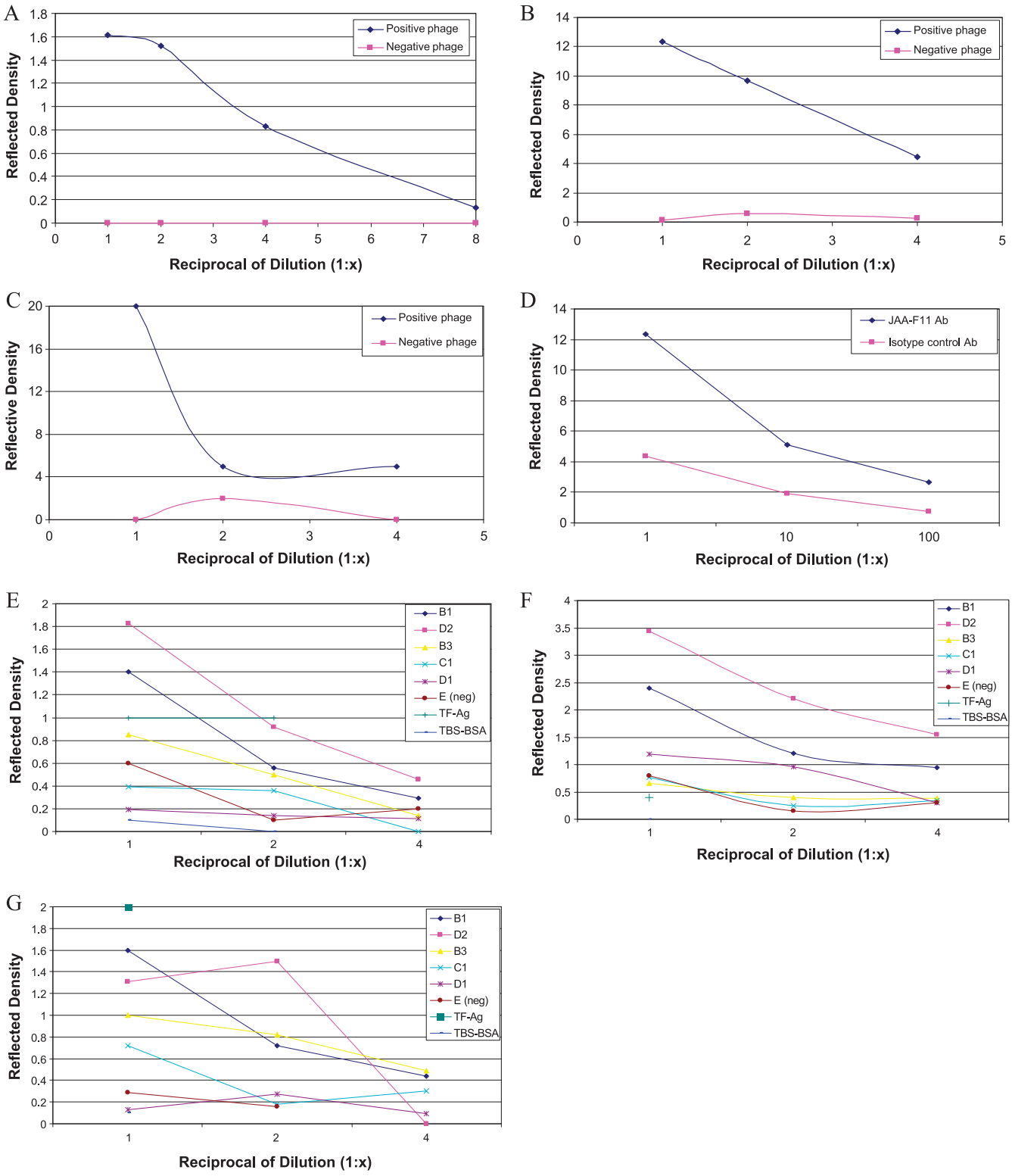

Figure 2. Immunoblot quantitation of bound pooled phage (A–D) and bound individual phage clones (E–G). (A–D) Pooled positive and negative phage (at 2.8×10^{10} and 2.2×10^{10} PFU/ml, respectively) were diluted 1:1, 1:2, 1:4, and 1:8. (E–G) Phage clones (B1, D2, B3, C1, D1, E) were diluted 1:1, 1:2, and 1:4 for probing with Ab. (A and E) JAA-F11 monoclonal Ab (20 μg/ml) reactivity. (B and F) Rabbit polyclonal sera to TF-Ag (1:50). (C and G) PNA lectin (200 μg/ml) reactivity. (D) JAA-F11 and an isotype matched control (IgG_3). Blots were quantitated by densitometry and reflected density of the spots represented on the *y*-axes. TF-Ag–BSA was used as a positive control; TBS-BSA was used as the negative control.

Table 2. Peptide Reactivity and Percent Inhibition of JAA-F11 Binding.

Name	Sequence of Selected Phage	% Inhibition	Reactivity with		
			JAA-F11	Rabbit Ab	PNA
D2	HIH GWK SPL SSL GGG S/C	49%	++	++	++
*B1	HHS HKT NLA TTP GGG S/C	21%	++	++	++
B3	GHP HYI THK PNR GGG S/C	21%	+	+/–	++
C1	YPS LPV YHS LRS GGG S/C	0	+/–	+/–	+
D1	MHK PWS GHM QVP GGG S/C	0	+/–	++	–
E	Negative phage pool	0	–	NT	NT

++ indicates strong binding; +, moderate binding; +/–, weak binding; –, no binding; *NT*, not tested.
*Relative reactivity of phage clones in immunoblots with JAA-F11, Rabbit Ab to TF-Ag, and PNA, a TF-Ag binding lectin, with phage are listed in order of reactivity with JAA-F11 in immunoblot. Sequence B1 was obtained three times; C2 and D3 also showed this sequence (not shown).

were sequenced. Three phage clones returned the same sequence (B1, C2, and D3), providing evidence of a good mimicking sequence, and additional four different sequences were obtained. These five sequences are listed in Table 2 as the 12-mer sequences followed by the next four residues present in the phage (GGGS). Of the five different sequences that were returned, the D2 phage reacted best in the immunoblots and inhibition ELISAs and was initially chosen as the focus of further studies.

BLAST Search

Using the National Center for Biotechnology Information BLAST database of known proteins, analysis was performed with the 15 amino acids that were input for the mimicking sequences (of which only the first 12 are considered part of the mimicking sequence), only partial matches were generated, with gaps in the compared sequences, which would not be likely to cross-react because the residues are not sequential. No 15/15 matches were generated for any of the five peptide mimic sequences. No significant findings were identified that would indicate similarity to other known proteins that would cause autoimmunity or tolerance *in vivo*.

In Vitro *Evidence of TF-Ag Mimicry by Selected Phage*

Peptide synthesis. Short single peptides corresponding to the 12–amino acid phage insert plus the 4–amino acid spacer were produced as 16-mer peptides. Cysteine was inserted in place of serine for ease of conjugation to carrier proteins. Eight peptides of the same sequences were linked to a 7-branched lysine core to produce MAP peptides (Figure 1) based on phage sequences that were found to act as mimics and a negative control MAP from Ova (SIINFEKLGAGAGGG).

In Vitro *Evidence of TF-Ag Mimicry by Synthetic Peptides*

Inhibition ELISAs. The purified D2 peptides were used in inhibition ELISA experiments as described in the previous sections. Inhibition, indicating specific binding, was seen with JAA-F11 Ab (up to 43%), rabbit Ab to TF-Ag (10%), and PNA (18%). These experiments show that D2 peptide is able to mimic TF-Ag by partially inhibiting the binding of Abs and a lectin known to bind TF-Ag with high specificity. When the B3 peptide was synthesized and tested with JAA-F11, it was also able to partially inhibit binding (50%). The levels of inhibition of rabbit Ab and PNA by D2 were not as high, likely because of the difference in affinity of the Ab for the univalent peptide *versus* the multivalent phage conjugate and multivalent TF-Ag conjugate, as the TF-Ag conjugate inhibited JAA-F11 Ab by 99% but only inhibited rabbit Ab by 62% and PNA by 14%.

Immunoblots. Immunoblots were performed as previously mentioned on peptides and were found to also bind JAA-F11 (data not shown).

Surface Plasmon Resonance

To determine the affinity of JAA-F11 Ab for a peptide mimic, SPR was performed using the Biacore system. An affinity, the K_D (M) for JAA-F11 binding to the single D2 peptide, was determined to be 5.73×10^{-4} M, in the submillimolar range of binding (Figure 3*A*).

In Vitro *Adhesion*

An *in vitro* adhesion system was used to demonstrate that peptide mimics, similar to TF-Ag [4] and Ab to TF-Ag [6], could block the adhesion of metastatic cancer cells to vascular endothelial cells, as a model of the *in vivo* mechanism of action. The D2 peptide was able to significantly inhibit rolling adhesion by approximately 43% and stable adhesion by approximately 71%, indicating that the binding of D2 peptide to the natural TF-Ag ligands on the vascular endothelium prevented TF-Ag expressed on the tumor cells from binding (Figure 3*B*). Importantly, when JAA-F11 Ab was used in this model system, it also significantly blocked rolling and stable adhesion of cancer cells to the endothelial cells [6]. *In vivo*, JAA-F11 significantly reduced metastasis of breast tumor cells, and the adhesion system provides a mechanism of action for JAA-F11 blocking the adhesion of cancer cells to metastatic sites [6]. Additional peptide mimics are currently being tested in this functional model system of adhesion.

MHC Prediction

Using MHC binding prediction databases, it was determined that the isolated peptide sequences are likely to be bound and presented by many MHC molecules, in both mouse and human and by both class I and class II molecules (data not shown). This indicates that peptides used in immunizations have the ability to be presented by MHC molecules to T cells for potential reactivity. Of the mice used in this study, the Balb/c strain harbors H2-^{d} MHC molecules and the C3H strain harbors H2-^{k} MHC. With regard to humans, the MHC molecules able to bind these peptides in the search are common human leukocyte antigen A and B (HLA-A and HLA-B) classes in the population, giving relevance to this search [51]. The MHC predictions are based on known binding algorithms and thus accurately reflect the ability of the peptide to bind and be presented *in vivo* in a large portion of the population, with additional *in vivo* support.

For relevance, the maximal scores given for these peptide mimics were compared with the scores found for another published peptide mimic of a carbohydrate tumor Ag, Lewis Y. This peptide mimic (GGIYWRYDIYWRYDIYWRYD) used in immunizations was shown to elicit IgM and IgG antibodies and to induce carbohydrate reactive T cells [25]. Therefore, the maximal binding scores to class I molecules of this peptide epitope were compared, and all MHC molecules listed are predicted to bind at least one peptide mimic. This information predicts that the peptides, when injected in mice, can be presented by at least several of the haplotypes present.

MAPs and Linear Peptides

After confirming the correct sequences of the MAPs and linear peptides by HPLC and mass spectrometry analyses, immunoblots

A

K_a (1/Ms)	K_d (1/s)	Rmax (RU)	K_A (1/M)	K_D (M)
232	0.133	548	1.75×10^3	5.73×10^{-4}

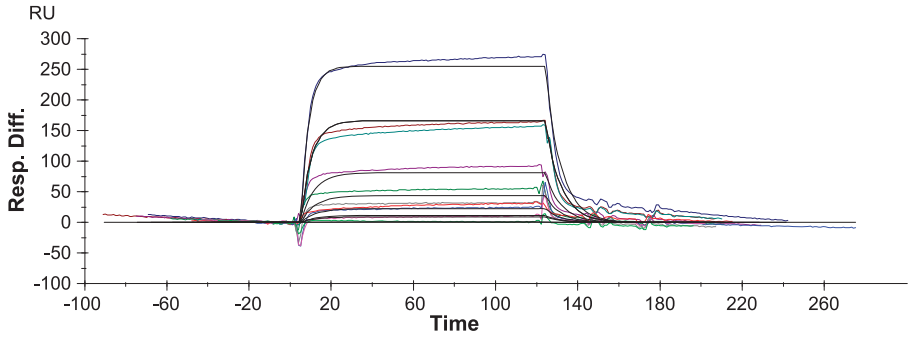

B

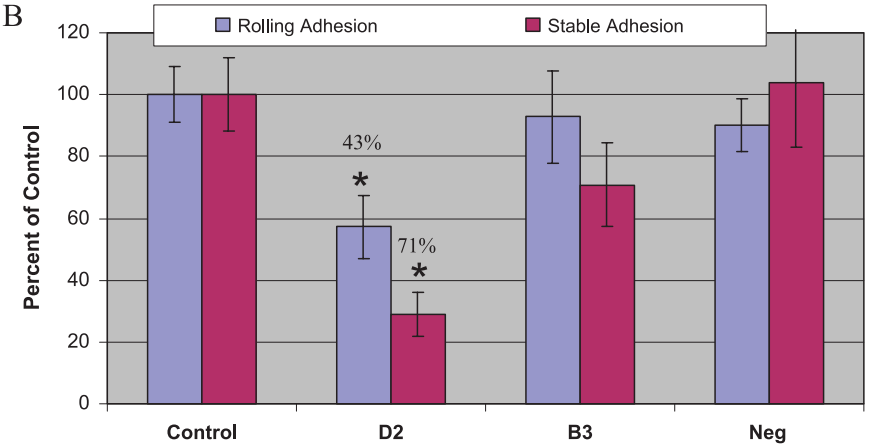

Figure 3. (A) Biacore (SPR) analysis of JAA-F11 binding to D2 peptide. Table shows binding kinetics for the binding of JAA-F11 to D2 peptide (using BiaEval software), and figure displays the range of D2 peptide concentrations binding to JAA-F11. JAA-F11 Ab coupled to a CM5 sensorchip was used to detect the binding of D2 to the Ab. The sensorgram graph is representative of several binding experiments, showing the dose–response of peptide binding to JAA-F11 *versus* time. (B) Two peptide mimics blocking rolling and stable adhesion of MD-MBA-235 human breast cancer cells to HBME-1 human bone marrow endothelial cells *in vitro*. Adhesion of MDA-MB-435 cells to HBME-1 cells using a parallel plate laminar flow chamber was assessed. The percent rolling MDA-MB-435 cells and number of stably adherent cells per field determined during 1- and 5-minute periods, respectively, in at least three different observation fields for each experimental setting. *Control* indicates no peptide; *Negative*, nonrelated peptide. Data are presented as mean ± SEM of two independent experiments. *D2 significant inhibition, corresponding to 43% inhibition of rolling and 71% inhibition of stable adhesion.

were performed to determine the reactivity with JAA-F11 Ab. JAA-F11 binding was seen to B1, D2, and C1 MAPs, whereas a lack of binding was seen to B3, D1, and Ova MAPs (data not shown). All five linear peptide mimicking sequences were found to bind to JAA-F11 under optimized experimental conditions (data not shown) and were used for the subsequent sera analyses.

Immunization

Serum analysis. Linear peptides corresponding to the same sequences used in the MAPs were used. The preimmunization (Pre), week 6, and week 8 sera were tested in triplicate at 1:200, 1:400, and 1:800 on linear peptide–coated plates (corresponding to the MAP used for immunization) as well as Ova linear peptide–coated plates for IgG and IgM Abs. This allowed for the determination of the levels of Ab made to the immunized peptide to ensure that the immunizations were successful in eliciting a robust immune response. Good immune responses toward the peptides were seen. This analysis also allowed for the detection of any Ab that reacted with the negative Ova peptide, which would indicate nonspecific Ab to any MAPs or to the lysine core, rather than specific Ab to the peptide sequences. No cross-reactive Ab between the peptides was seen (data not shown). The Pre, week 6, and week 8 sera were tested at 1:50 in triplicate on TF-Ag–BSA–coated plates for IgG and IgM Abs. These assays yielded measurable levels of specific Ab without high levels of background binding in the sera. To determine whether an early immune response occurred, which was missed, 33 additional mice were vaccinated, and their sera were obtained on day 7. The sera from the 7-day study were tested in triplicate at 1:50 on TF-Ag– and linear peptide–coated plates for IgG and IgM Abs. At 7 days, the levels of IgM Ab might be expected to be higher than at day 14. However, little Ab response, IgG, or IgM was seen at this time point (data not shown).

Statistical analyses. The Abs produced to immunized peptide and the control Ova peptide were compared using the same dilutions as previously mentioned to compare the responses to the different peptides. Screening of sera from six mice per group was analyzed, showing that D2, B3, C1, and Ova peptides caused production of greater

amounts of Ab; D1, B1, and the mixture of peptides caused moderate production of Ab; and PBS alone did not result in Ab production.

The anti–TF-Ag response was tested with sera at a 1:50 dilution. Statistically significant increases from preimmunization to postimmunization were seen within each group (Figure 4, *A–D*) showing that the immunization protocol was effective in eliciting an immune response by itself because increases were seen in the negative groups as well. Comparisons between groups were also made (Figure 4, *E–H*). Both IgG and IgM productions were tested. These dot plots allow for the distribution of the responses in each group to be seen as well as the mean of each group. Table 3 summarizes this information.

Additional line graphs visualize the response trends over the time points tested in each group. To further and more accurately analyze the Ab response, a more complex statistical analysis was performed, as explained previously. This model allowed for the consideration of different baseline levels of Ab and statistically compared the differences among groups using more stringent constraints. Therefore, fewer groups showed a significant response over the controls groups by this analysis. For IgG Ab to TF-Ag, statistically significant results were found between B1 and each of the control groups at both the 6- and 8-week time points ($P < .0001$; Figure 5*A*). All other comparisons with the control groups were found to be nonsignificant. For IgM Ab to TF-Ag, statistically significant results were found between C1 and Ova ($P = .0312$) and between C1 and PBS ($P = .0012$) at the 6-week time point. At the 8-week time point, significant differences were found between C1 and Ova ($P = .0007$), C1 and PBS ($P < .0001$), and B1 and PBS ($P = .0016$; Figure 5*B*). All other comparisons with the control groups were found to be nonsignificant. Whereas fewer groups were found to be significant, the stringency of this model suggests that the groups that are significant are representing a true and valid anti–TF-Ag response to the peptide mimics.

The previously mentioned analyses at 1:50 consider each group as a whole by averaging the group responses and then performing analyses. However, individual mouse responses can vary, and therefore, examining the responses of individual mice was performed. The most accurate method to analyze each mouse singly was to quantitate the absolute change in OD, correcting for the differences in baseline Ab levels among mice. The absolute changes in OD for IgG and IgM Abs for each mouse were determined and represented as individual points on a dot plot (Figure 4, *A–H*). The percentage of mice in each group, which changed by a given amount, was counted. At the 0.2 OD change cut point, definite differences between groups are seen. For IgG Ab to TF-Ag, B1, C1, and D1 groups all have percentages of mice that are considerably higher than those in control Ova and PBS groups. B3, D2, and Mix groups, although not as high as B1, C1, and D1 groups, still have double the number of mice that responded with greater than 0.2 OD change over the negative groups (Figure 6*A*). For IgM Ab to TF-Ag, B1, C1, and D1 groups all have

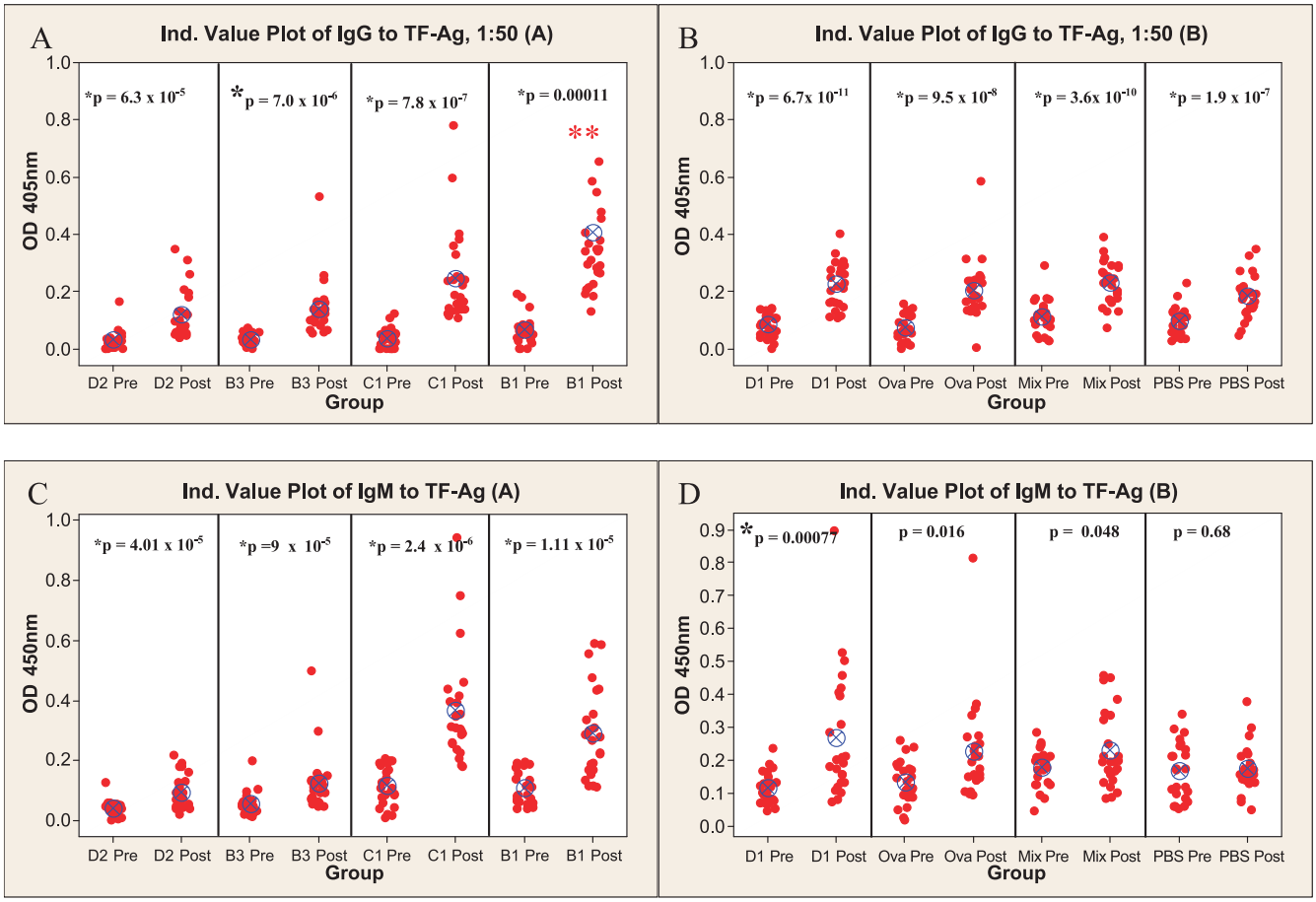

Figure 4. (A–H) Dot plots of all mice at 1:50, IgG and IgM to TF-Ag, at the same scale. Significance marked: **P*, difference from Pre to Post, mean = ⊗. (A an B) IgG to TF-Ag, all mice. (C and D) IgM to TF-Ag, all mice. (E) Pre and (F) Post bleed IgG to TF-Ag levels for all groups, respectively, to visualize the difference in the baseline (E) and response (F) levels between groups. (G) Pre and (H) Post bleed IgM to TF-Ag levels for all groups, respectively, to visualize the difference in the baseline (G) and response (H) levels between groups.

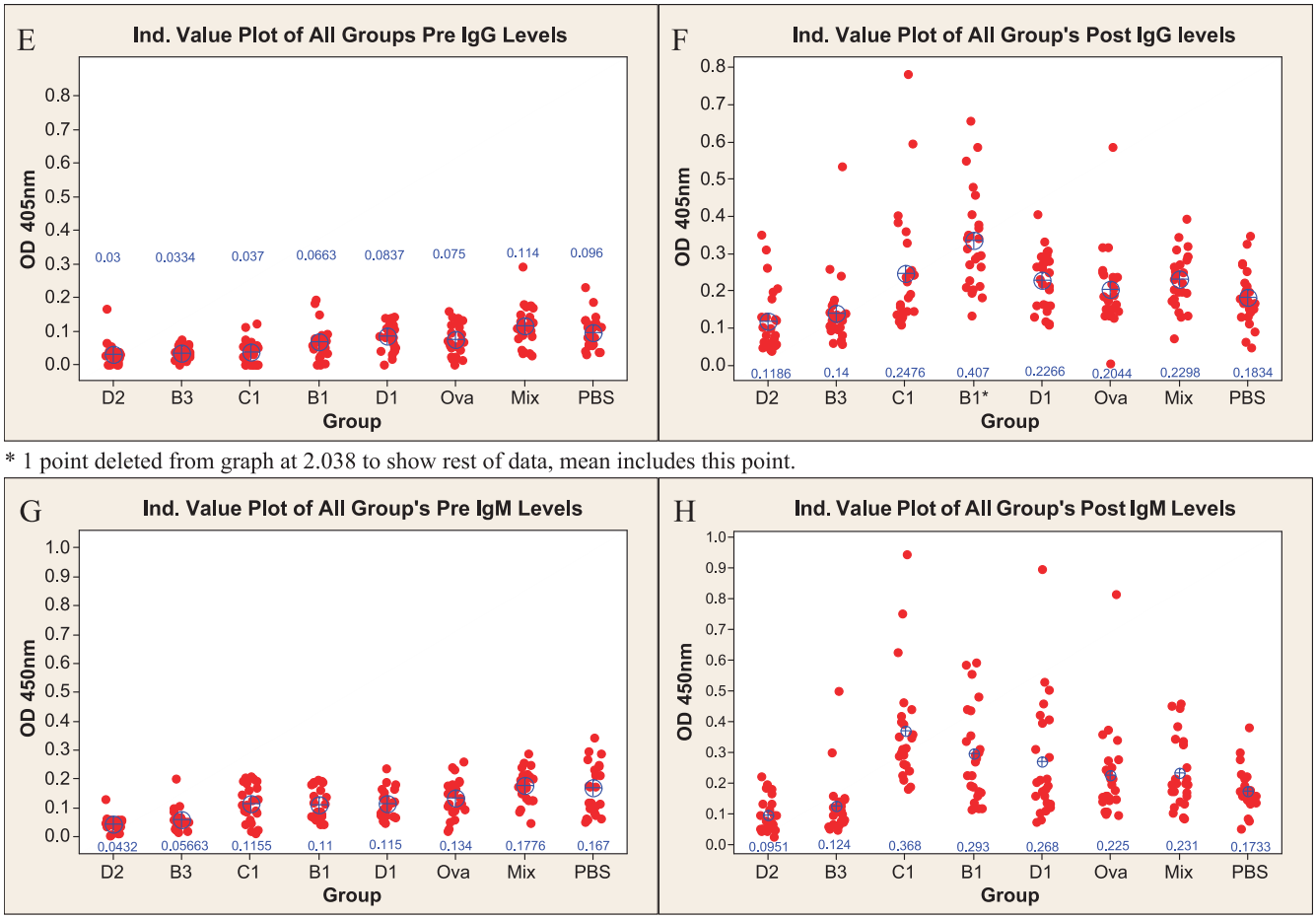

Figure 4. (*continued*)

Table 3. Immunized Sera Tested for Production of Reactive Ab to TF-Ag (1:50 Dilution).

Group: Pre *vs* Post	Significance: IgG to TF-Ag ($P < .05$)	Fold Increase in OD from Pre to Post	Significance: IgM to TF-Ag ($P < .05$)	Fold Increase in OD from Pre to Post
D2	1.48×10^{-6}	4-fold	4.02×10^{-5}	2.2-fold
B3	7.03×10^{-6}	4.2-fold	8.98×10^{-5}	2.2-fold
C1	7.78×10^{-7}	6.7-fold	2.44×10^{-6}	3.2-fold
B1	1.05×10^{-4}	7.5-fold	1.11×10^{-5}	2.7-fold
D1	6.67×10^{-11}	2.7-fold	7.74×10^{-4}	2.3-fold
Ova	9.47×10^{-8}	2.7-fold	.0155	1.67-fold
Mix	3.56×10^{-10}	2-fold	.048	1.3-fold
PBS	1.86×10^{-7}	1.9-fold	.68	0

Groups: (Post *vs* Post)	Significance: IgG to TF-Ag ($P < .05$)	Fold Increase from Post to Post	Significance: IgM to TF-Ag ($P < .05$)	Fold Increase in OD from Pre to Post
D2 *vs* Ova	NS	NS	NS	NS
D2 *vs* PBS	NS	NS	NS	NS
B3 *vs* Ova	NS	NS	NS	NS
B3 *vs* PBS	NS	NS	NS	NS
C1 *vs* Ova	.178	1.24-fold	.007	1.64-fold
C1 *vs* PBS	.093	1.35-fold	5.7×10^{-5}	2.16-fold
B1 *vs* Ova	.013	2-fold	.18	1.3-fold
B1 *vs* PBS	.005	2.18-fold	.002	1.7-fold
D1 *vs* Ova	.42	1.14-fold	.404	1.2-fold
D1 *vs* PBS	.04	1.24-fold	.036	1.6-fold
Mix *vs* Ova	.29	1.15-fold	.87	1.02-fold
Mix *vs* PBS	.057	1.26-fold	.049	1.35-fold
Ova *vs* PBS	.45		.18	

Using Student's *t* test (paired) to determine significance between Pre and Post (using the highest value of bleed 3 or 4) and Post to Post in each group, and the averages of each group used. No statistical calculations were used to compare fold differences in this case. Insignificant values for D2 and B3 partially reflect the lower baseline level in these groups compared with the controls.
NS indicates not significant.

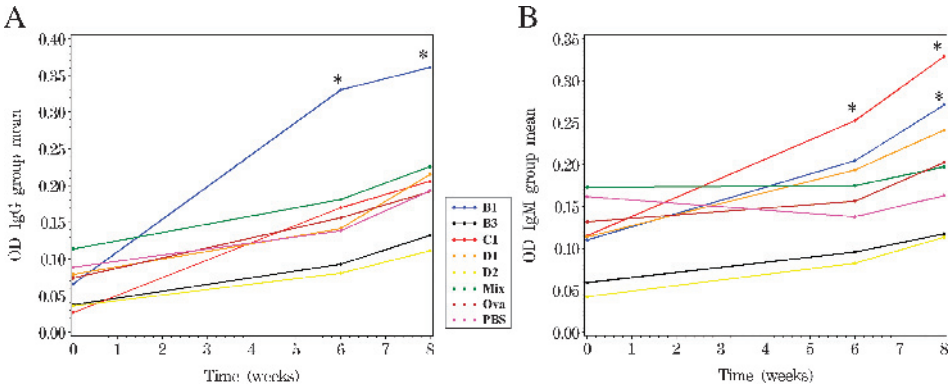

Figure 5. IgG (A) and IgM (B) line graphs of the average Ab level to TF-Ag tested at 1:50 of all mice in each group during three time points. Statistically significant results were found between B1 and each of the control groups (Ova and PBS) at both time points ($P < .0001$). All other comparisons with the control groups were found to be nonsignificant. At time point 6, statistical significant results were found between C1 and Ova ($P = .0312$) and between C1 and PBS ($P = .0012$). At time point 8, significant differences were found between C1 and Ova ($P = .0007$), between C1 and PBS ($P < .0001$), and between B1 and PBS ($P = .0016$). All other comparisons with the control groups were found to be nonsignificant.

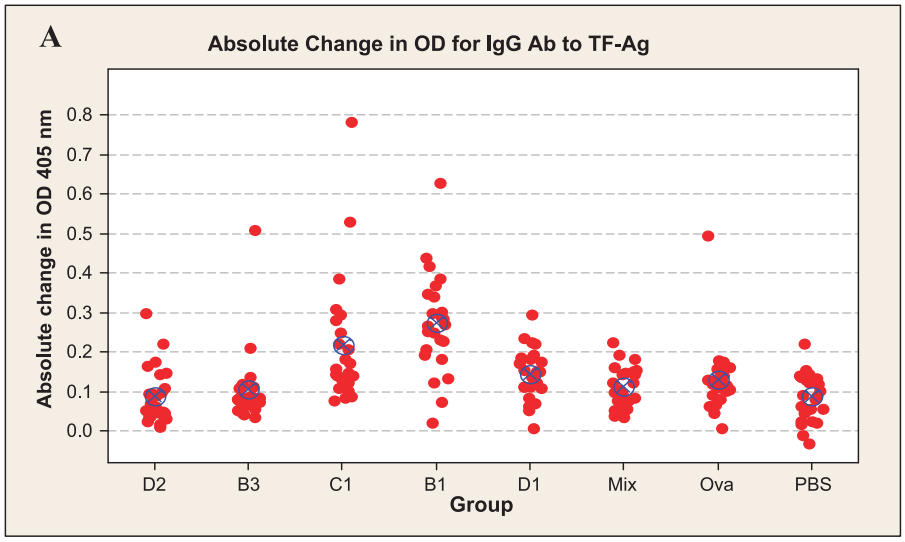

IgG Ab response, based on absolute change in OD by group.

Group	Above 0.05 cutpoint	Above 0.10 cutpoint	Above 0.15 cutpoint	Above 0.20 cutpoint
B1	96%	92%	84%	76%
B3	88%	36%	12%	8%
C1	100%	84%	60%	36%
D1	96%	80%	40%	16%
D2	56%	28%	16%	8%
Mix	88%	52%	24%	8%
Ova	92%	76%	24%	4%
PBS	84%	56%	12%	4%
p values for significant pairwise differences (control vs. peptide)			Ova/B1 0.0005 PBS/B1 <0.0001 PBS/C1 0.0109	Ova/B1 <0.0001 PBS/B1 <0.0001

Figure 6. (A) Absolute changes in OD for IgG Ab to TF-Ag in each mouse per group, mean = ⊗. (B) Absolute changes in OD for IgM Ab to TF-Ag in each mouse per group, mean = ⊗.

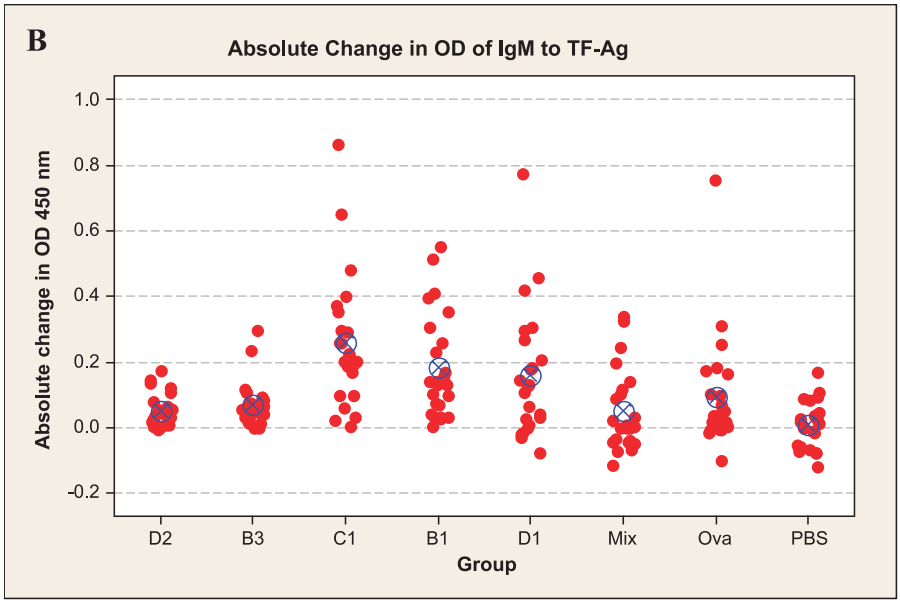

IgM Ab response, based on absolute change in OD by group.

Group	Above 0.05 cutpoint	Above 0.10 cutpoint	Above 0.15 cutpoint	Above 0.20 cutpoint
B1	80%	64%	40%	32%
B3	48%	16%	8%	8%
C1	88%	72%	72%	52%
D1	60%	52%	36%	28%
D2	44%	24%	8%	4%
Mix	36%	32%	16%	12%
Ova	36%	28%	24%	12%
PBS	20%	8%	4%	0%
p values for significant pairwise differences (control vs. peptide)	Ova/B1 0.0440 Ova/C1 0.0040 PBS/B1 0.0006 PBS/C1 <0.0001	PBS/B1 0.0009 PBS/C1 0.0001 PBS/D1 0.0179	Ova/C1 0.0188 PBS/C1 <0.0001	PBS/B1 0.0484 PBS/C1 0.0004

Figure 6. (*continued*)

percentages of mice that are considerably higher than the control Ova and PBS groups. B3, D2, and Mix groups have comparable numbers of mice that responded with greater than 0.2 OD change compared with the negative groups (Figure 6*B*). Considering the fact that B1, C1, and D1 groups have appreciably more mice with 0.2 OD change in Ab levels and the cut points used in this analysis, these data suggest that these groups contain mice that exhibited significant responses, representing true and valid responses to peptide mimics.

Discussion

In this study, we have used TF-Ag, which is a pan-carcinoma tumor cell surface carbohydrate Ag, as the target for an immune response. By developing peptide mimics of the carbohydrate structure for use in vaccines, it is anticipated that we can begin a process that will ultimately result in a clinically relevant immune response to TF-Ag epitope-expressing tumor cells.

Through several methods of *in vitro* characterization of selected peptides, it was shown that mimicry of TF-Ag occurs. Abs to TF-Ag, both mouse monoclonal and rabbit polyclonal, as well as PNA lectin known to bind TF-Ag, bound to the peptide mimics as well. The peptides partially inhibited the binding of TF-Ag Abs to TF-Ag disaccharide-protein conjugates by ELISA. The D2 peptide significantly inhibited stable and rolling adhesion of TF-Ag epitope-expressing tumor cells to human endothelial cells. These data may offer a potential mechanism for Ab generated toward TF-Ag *in vivo* in blocking cell-cell adhesion and thus prevent metastasis to distant sites.

The peptide mimics may further function to stimulate an immune reaction that responds to TF-Ag epitope-expressing tumor cells. BLAST analysis showed that an immune response to these peptides should not cause an autoimmune reaction, and MHC binding prediction analysis showed that these peptides are likely to be presented.

To achieve successful peptide mimic immunizations, Ab that binds TF-Ag should be produced. Four different analyses were used to ensure comprehensive characterization of the Ab responses, as seen in some peptide mimic-immunized groups, albeit low levels. Statistically significant increases in Ab levels were seen from preimmunization to postimmunization sera. This is an important result, showing that it

is possible to create Ab to TF-Ag peptide mimics, which reacts with TF-Ag itself. Each peptide elicited varying levels of response, signifying that not all peptides are equal mimics *in vivo*. This was not unexpected, given that the peptides do differ greatly in sequence and therefore chemical character. It is also not surprising that the peptides behave differently in *in vitro* assays than in the *in vivo* environment. Because of these differences, it was important to immunize with all of the potential peptide mimics regardless of their *in vitro* activity. B1, which did not react highly with JAA-F11 Ab *in vitro*, displayed the highest immunogenic response *in vivo*. Peptide immunizations produced moderate to high levels of Ab reactive with the immunized peptide itself, showing that the peptide immunogenicity was adequate, and any lack of TF-Ag Ab was not due to suboptimal immunization conditions. There was little to no cross-reactivity with the negative Ova peptide, showing that Ab responses were peptide sequence-specific. Little to no Ab was seen at 1-, 2-, and 4-week time points, but at the 6- and 8-week time points, significant Ab levels were generated. The most promising peptide before the *in vivo* immunizations was D2. The lack of success of this peptide MAP led to subsequent studies that showed that the D2 peptide is relatively unstable, thus the peptide could have been modified or broken down during the course of the immunization protocol and not able to sufficiently act as a mimic *in vivo*. This eventual loss of reactivity seen after long-term storage was due to the apparent oxidative modifications to the peptide. This corresponded to a change in the molecular weights of the peptide as demonstrated by matrix-assisted laser desorption/ionization–time of flight (data not shown). One modification was an increase of 32 in the molecular weight, which could be attributed to addition of two oxygen atoms to the peptide by oxidative reactions. Subsequent electrospray ionization–mass spectrometry analysis suggested that either the tryptophan or proline residue of the D2 peptide was modified (data not shown), suggesting that either of these residues is critical for binding.

These results, showing Ab reactive to TF-Ag after peptide immunizations, is encouraging for the use of peptide mimics. The fact that IgG Abs were generated is a positive sign of T-cell involvement, and T-cell immunity relative to carbohydrates has attracted great attention in recent years [52]. If the response to TF-Ag peptide mimics can be increased using better peptide mimics or other improved techniques to generate higher levels of TF-Ag–reactive Ab with T-cell involvement, this research would have greater applicability. The creation of an immune response to TF-Ag through peptide mimics can be used to decrease the tumor burden of cancer patients, concurrent with leading treatments. The added benefits of this technique include the ability to differentially target TF-Ag–positive tumor cells and block metastatic adhesion through the development of Ab to the specific carbohydrate Ag.

The current data illuminating the development and characterization of peptide mimics of TF-Ag provide *in vitro* support for the functionality of these mimics and continued study of mimics for vaccine development directed at TF-Ag epitope-expressing tumor cells. On further studies to improve the peptides, including crystallization and modeling analysis, vaccination schemes using peptide mimics have the ability to be applied for the prevention of recurrence of TF-Ag epitope-expressing adenocarcinomas by generating an immune response that targets and blocks TF-Ag. The widespread applicability of the use of peptide mimics of TF-Ag makes it a significant area of research for further exploration. Owing to the importance of breaking tolerance to TF-Ag, a second vaccine approach will be attempted, which will use constructs containing TF-Ag mimicking peptides linked to the mucin-1 peptide and additionally linked to one or more immune-enhancing agents including C3d, the T-cell–stimulating peptides, zwitterionic constructs, and Toll-like receptor agonists. The peptides will facilitate effective T helper cell response, reacting with multiple HLA molecules. C3d will facilitate activation of B cells without T-cell help by targeting CD21, the C3d receptor, on splenic marginal zone B cells, and follicular dendritic cells [53]. Zwitterions will generate Toll-like receptor agonists, and these will facilitate uptake and activation of Ag-presenting cells [54,55]. These additional vaccine strategies could improve the immunogenicity of the peptide mimics toward the TF-Ag tumor epitope.

Acknowledgments

The authors thank Brian Lang for aiding in the Biacore analysis, Chad Vezina for help in the phage sequencing method, Adrian Grozav for electrospray ionization–mass spectrometry analysis, and Stephen Koury for use of the slot blot apparatus.

References

[1] Springer GF (1984). T and Tn, general carcinoma autoantigens. *Science* **224**, 1198–1206.
[2] Irazoqui FJ and Nores GA (2003). Thomsen-Friedenreich disaccharide immunogenicity. *Curr Cancer Drug Targets* **3**, 433–443.
[3] Rittenhouse-Diakun K, Xia Z, Pickhardt D, Morey S, Baek M-G, and Roy R (1998). Development and characterization of monoclonal antibody to T-antigen (Galβ1-3GalNAcα-O). *Hybridoma* **17-2**, 165–173.
[4] Glinsky VV, Glinsky GV, Rittenhouse-Olson K, Huflejt ME, Glinskii OV, Deutscher SL, and Quinn TP (2001). The role of Thomsen-Friedenreich antigen in adhesion of human breast and prostate cancer cells to the endothelium. *Cancer Res* **61**, 4851–4857.
[5] Howard DR, Ferguson P, and Batsakis JG (1981). Carcinoma-associated cytostructural antigenic alterations. Detection by lectin binding. *Cancer* **47**, 2872–2877.
[6] Heimburg J, Yan J, Morey S, Glinskii OV, Huxley VH, Wild L, Klick R, Roy R, Glinsky VV, and Rittenhouse-Olson K (2006). Inhibition of spontaneous breast cancer metastasis by Thomsen-Friedenreich antigen monoclonal antibody JAA-F11. *Neoplasia* **8**, 939–948.
[7] Yu LG (2007). The Thomsen-Friedenreich carbohydrate antigen in epithelial cancer progression. *Glycoconj J* **24**, 411–420.
[8] Springer GF (1995). T and Tn pancarcinoma markers autoantigenic adhesion molecules in pathogenesis, prebiopsy carcinoma detection, and long term breast carcinoma immunotherapy. *Crit Rev Oncog* **6**, 57–85.
[9] Rahman AF and Longenecker BMA (1982). Monoclonal antibody specific for the Thomsen-Friedenreich cryptic antigen. *J Immunol* **129**, 2021–2025.
[10] Springer GF and Desai PR (1975). Blood group MN antigens and precursors in normal and malignant human breast glandular tissue. *J Natl Cancer Inst* **54**, 335–339.
[11] Hakomori S (1984). Tumor-associated carbohydrate antigens. *Annu Rev Immunol* **2**, 103–126.
[12] Friedenreich V (1930). *The Thomsen Hemagglutination Phenomenon.* Copenhagen, Denmark: Levin and Munksgaard.
[13] Klaamas K, Kurtenkov O, von Mensdorff-Pouilly S, Shljapnikova L, Miljukhina L, Brjalin V, and Lipping A (2007). Impact of *Helicobacter pylori* infection on the humoral immune response to MUC1 peptide in patients with chronic gastric diseases and gastric cancer. *Immunol Invest* **36**, 371–386.
[14] Springer GF (1997). Immunoreactive T and Tn epitopes in cancer diagnosis, prognosis, and immunotherapy. *J Mol Med* **75**, 594–602.
[15] O'Boyle KP, Zamore R, Adluri S, Cohen A, Kemeny N, Welt S, Lloyd KO, Oettgen HF, Old LJ, and Livingston PO (1992). Immunization of colorectal cancer patients with modified ovine submaxillary gland mucin and adjuvant induces IgM and IgG antibodies to sialylated Tn. *Cancer Res* **52**, 5663–5667.
[16] O'Boyle KP, Markowitz AL, Khorshidi M, Lalezari P, Longenecker BM, Lloyd KO, Welt S, and Wright KE (1996). Specificity analysis of murine monoclonal antibodies reactive with Tn, sialylated Tn, and monosialylated (2-6) T antigens. *Hybridoma* **15**, 401–408.

[17] Holmberg LA and Sandmaier BM (2001). Theratope vaccine (STn-KLH). *Expert Opin Biol Ther* **1**, 881–891.

[18] Gilewski T, Ragupathi G, Bhuta S, Williams LJ, Musselli C, Zhang XF, Bornmann WG, Spassova M, Bencsath KP, Panageas KS, et al. (2001). Immunization of metastatic breast cancer patients with a fully synthetic globo H conjugate: a phase I trial. *Proc Natl Acad Sci USA* **98**, 3270–3275.

[19] Pincus SH, Smith MJ, Jennings HJ, Burritt JB, and Glee PM (1998). Peptides that mimic the group B streptococcal type III capsular polysaccharide antigen. *J Immunol* **160**, 293–298.

[20] Grothaus MC, Srivastava N, Smithson SL, Kieber-Emmons T, Williams DB, Carlone GM, and Westerink MA (2000). Selection of an immunogenic peptide mimic of the capsular polysaccharide of *Neisseria meningitidis* serogroup A using a peptide display library. *Vaccine* **18**, 1253–1263.

[21] Irving MB, Pan O, and Scott JK (2001). Random-peptide libraries and antigen-fragment libraries for epitope mapping and the development of vaccines and diagnostics. *Curr Opin Chem Biol* **5**, 314–324.

[22] Kieber-Emmons T, Monzavi-Karbassi B, Wang B, Luo P, and Weiner DB (2001). Cutting edge: DNA immunization with minigenes of carbohydrate mimitopes induce functional anti-carbohydrate antibody response. *J Immunol* **165**, 623–627.

[23] Luo P, Agadjanyan M, Qiu J, Westerink MJ, Steplewski Z, and Kieber-Emmons T (1998). Antigenic and immunological mimicry of peptide mimitopes of Lewis carbohydrate antigens. *Mol Immunol* **35**, 865–879.

[24] Monzavi-Karbassi B, Cunto-Amesty G, Luo P, and Kieber-Emmons T (2002). Peptide mimotopes as surrogate antigens of carbohydrates in vaccine discovery. *Trends Biotechnol* **20**, 207–214.

[25] Monzavi-Karbassi B, Cunto-Amesty G, Luo P, Lees A, and Kieber-Emmons T (2001). Immunological characterization of peptide mimetics of carbohydrate antigens in vaccine design strategies. *Biologicals* **29**, 249–257.

[26] Shikhman AR and Cunningham MW (1997). Trick or treat: toward peptide mimic vaccines. *Nat Biotechnol* **15**, 512–513.

[27] Cunto-Amesty G, Luo P, Monzavi-Karbassi B, Lees A, and Kieber-Emmons T (2001). Exploiting molecular mimicry to broaden the immune response to carbohydrate antigens for vaccine development. *Vaccine* **19**, 2361–2368.

[28] Johnson MA, Jaseja M, Zou W, Jennings H, Copié V, Pinto BM, and Pincus SH (2003). NMR studies of carbohydrates and carbohydrate-mimetic peptides recognized by an anti–group B *Streptococcus* antibody. *J Biol Chem* **278**, 24740–24752.

[29] Vyas NK, Vyas MN, Chervenak MC, Bundle DR, Pinto BM, and Quiocho FA (2003). Structural basis of peptide-carbohydrate mimicry in an antibody-combining site. *Proc Natl Acad Sci USA* **100**, 15023–15028.

[30] Hossany RB, Johnson MA, Eniade AA, and Pinto BM (2004). Synthesis and immunochemical characterization of protein conjugates of carbohydrate and carbohydrate-mimetic peptides as experimental vaccines. *Bioorg Med Chem* **12**, 3743–3754.

[31] *12 Phage Display Peptide Library Kit Instruction Manual, Version 2.5*. New England Biolabs, Inc, PhD, Beverly, MA. Available from: http://www.neb.com/nebecomm/products/productE8110.asp. Accessed March 13, 2002.

[32] *Phage Display* (2004). Dyax Corporation, Cambridge, MA. Available from: http://www.dyax.com/discovery/index.html. Accessed September 18, 2002.

[33] Diakun KR, Yazawa S, Abbas SA, and Matta KL (1987). Synthetic antigens as immunogens: Part II. Antibodies to synthetic T antigen. *Immunol Invest* **16**, 151–163.

[34] Chaturvedi R, Yan J, Heimburg J, Koury S, Sajjad M, and Rittenhouse-Olson K (2008). Immuno-PET and biodistribution using iodine-124 labeled anti–Thomsen-Friedenreich–antigen monoclonal antibody JAA-F11. *Appl Radiat Isot* **66**, 278–287.

[35] Doyle K (1996). *Protocols and Applications Guide, Biological Research Products Manual.* 3rd Ed. Madison, WI: Promega Corporation.

[36] Roe B. *DNA Purification from M13 Phage*. University of Oklahoma Advanced Center for Genome Technology, Norman, OK. Available from: http://www.genome.ou.edu/protocol_book/protocol_partIII.html#III.E. Accessed March 18, 2002.

[37] Fields GB and Noble RL (1990). Solid-phase peptide-synthesis utilizing 9-fluorenylmethoxycarbonyl amino-acids. *Int J Pept Protein Res* **35**, 161–214.

[38] Chan WC and White PD (2000). *Fmoc SPPS: A Practical Approach.* New York, NY: Oxford University Press.

[39] Dziadek S, Brocke C, and Kunz H (2004). Biomimetic synthesis of the tumor-associated (2,3)-sialyl-T antigen and its incorporation into glycopeptide antigens from the mucins MUC1 and MUC4. *Chem – A Eur J* **10**, 4150–4162.

[40] Cremer G, Bureaud N, Piller V, Kunz H, Piller F, and Delmas AF (2006). Synthesis and biological evaluation of a multiantigenic Tn/TF–containing glycopeptide mimic of the tumor-related MUC1 glycoprotein. *ChemMedChem* **1**, 965–968.

[41] Stenberg E, Persson B, Roos H, and Urbaniczky C (1991). Quantitative determination of surface concentration of protein with surface plasmon resonance by using radiolabeled proteins. *J Colloid Interface Sci* **143**, 513–526.

[42] Karlsson R and Falt A (1997). Experimental design for kinetic analysis of protein-protein interactions with surface plasmon resonance biosensors. *J Immunol Methods* **200**, 121–133.

[43] Lehr JE and Pienta KJ (1998). Preferential adhesion of prostate cancer cells to a human bone marrow endothelial cell line. *J Natl Cancer Inst* **90**, 118–123.

[44] National Comprehensive Cancer Network (2005). *Clinical Practice Guidelines for Breast Cancer, Version 2.* National Comprehensive Cancer Network, Fort Washington, PA. Available from: http://www.nccn.org/professionals/physician_gls/PDF/breast.pdf.

[45] Rammensee H-G, Bachmann J, Emmerich NN, Bachor OA, and Stevanovic S (1999). SYFPEITHI: database for MHC ligands and peptide motifs. *Immunogenetics* **50**, 213–219; Available from: www.syfpeithi.de. Accessed June 5, 2006.

[46] Parker KC, Bednarek MA, and Coligan JE (1994). Scheme for ranking potential HLA-A2 binding peptides based on independent binding of individual peptide side-chains. *J Immunol* **152**, 163; Available from: http://bimas.dcrt.nih.gov/molbio/hla_bind/. Accessed June 5, 2006.

[47] Reche PA, Glutting JP, and Reinherz EL (2002). Prediction of MHC class I binding peptides using profile motifs. *Hum Immunol* **63**, 701–709; Available from: http://mif.dfci.harvard.edu/Tools/rankpep.html. Accessed June 5, 2006.

[48] National Center for Biotechnology Information. *Basic Local Alignment Search Tool (BLAST), Version 2.2.15*. National Center for Biotechnology Information, Bethesda, MD. Available from: http://www.ncbi.nlm.nih.gov/BLAST/. Additional information: http://www.ncbi.nlm.nih.gov/books/bv.fcgi?rid=handbook.chapter.ch16. Accessed June 19, 2006.

[49] Cribbs DH, Ghochikyan A, Vasilevko V, Tran M, Petrushina I, Sadzikava N, Babikyan D, Kesslak P, Kieber-Emmons T, Cotman CW, et al. (2003). Adjuvant-dependent modulation of T_H1 and T_H2 responses to immunization with β-amyloid. *Int Immunol* **15**, 505–514.

[50] Maruta T, Oshima M, Deitiker PR, Ohtani M, and Atassi MZ (2006). Use of alum and inactive *B. pertussis* for generation of antibodies against synthetic peptides in mice. *Immunol Invest* **35**, 137–148.

[51] Robinson J, Bodmer JG, Malik A, and Marsh SGE (1998). Development of the International Immunogenetics HLA database. *Hum Immunol* **59**, 17.

[52] Icart LP, Santana VF, and Bencomo VV (2008). T-cell immunity of carbohydrates. In R Roy (Ed.). *Carbohydrate-Based Vaccines ACS Symposium Series 989*. American Chemical Society, Washington, DC.

[53] Dempsey PW, Allison MED, Akkaraju S, Goodnow CC, and Fearon DT (1996). C3d of complement as a molecular adjuvant: bridging innate and acquired immunity. *Science* **271**, 348–356.

[54] Gallorini S, Berti F, Parente P, Barononio R, Aprea S, D'Oro U, Pizza M, Telford JL, and Wack A (2007). Introduction of zwitterionic motifs into bacterial polysaccharides generates TLR2 agonists able to activate APCs. *J Immunol* **179**, 8208–8215.

[55] Ingale S, Wolfert MA, Gaekwad J, Buskas T, and Boons G-J (2007). Robust immune responses elicited by a fully synthetic three-component vaccine. *Nat Chem Bio* **3**, 663–667.